2023 IEEE 66th International Midwest Symposium on Circuits and Systems (MWSCAS)
Phoenix, Arizona, USA, August 6-9, 2023

Investigating R(t) Functions for Spike-Timing-Dependent Plasticity in Memristive Neural Networks

Farhana Afrin, Kurtis D. Cantley, Department of Electrical and Computer Engineering, Boise State University Boise, ID 83725, United States, farhanaafrin@u.boisestate.edu, kurtiscantley@boisestate.edu

2023 IEEE 66th International Midwest Symposium on Circuits and Systems (MWSCAS) | 979-8-3503-0210-3/23/$31.00 ©2023 IEEE | DOI: 10.1109/MWSCAS57524.2023.10405895

Abstract— **Brain-inspired neuromorphic computation can be extremely efficient at very large scales due to inherent parallelism, scalability, and fault and failure tolerance. One widely used, biologically plausible synaptic learning mechanism is spike-timing-dependent plasticity (STDP). The proposed generic model of time-varying resistance, or R(t) elements in this work, can produce classical and beyond classical STDP in electronic spiking neural networks with memristive synapses. Hebbian and Anti-Hebbian STDP is verified with the proposed generic R(t) model by tuning the R(t) function. By appropriately placing R(t) functions with selective resistance values, symmetric or non-classical STDP learning behavior is achieved.**

Keywords—Spike-Timing-Dependent Plasticity, R(t) element, memristor, Spiking Neural Network, Hebbian, Anti-Hebbian.

I. Introduction

Memristive Spiking Neural Networks (SNNs) that mimic the Spike-Timing-Dependent Plasticity (STDP) learning rule are potential candidates for energy-efficient brain-inspired computation [1-4]. Different forms of the STDP rule depend on dendritic position, the nonlinear integration of synaptic modulation induced by complex spike trains, and the alteration by inhibitory and neuromodulator inputs [5-12]. Moreover, multiple studies reveal that calcium-based plasticity in hippocampal culture and the visual cortex regions in the brain depend on both spike rate and timing [13-17]. In classical pair-based STDP, the weight change caused by a positive temporal difference (pre-synaptic neuron firing before post-synaptic neuron) is positive. Similarly, the weight change caused by a negative temporal difference (post-synaptic neuron firing before pre-synaptic neuron) is negative and different from the positive weight change, i.e., asymmetric [18]. In parts of the hippocampus and neocortex, learning rules other than classical STDP are observed, which can play crucial roles in the formation of new memories, processing of sensory information, and cognitive functions such as perception and decision-making [13,19-21].

Previously, some non-classical STDPs have been demonstrated using passively-integrated 1T1R (One Transistor-One Resistor) synaptic elements [14,16]. However, these approaches require additional pulse-shaping circuits. It is also challenging to create a single synaptic device with appropriate first and second-order responses for use in memristive neural networks [22, 23]. Adding relatively simple circuits to each neuron that can be altered to deliver the appropriate learning response depending on the specific characteristics of the memristive device is a considerably better solution. A time-dynamic resistance element is one example of such a circuit, which modulates the voltage across the synaptic memristor in a complex manner. R(t) elements could be devices such as short-term charge-trapping memories [17] or CMOS circuits [24]. In the CMOS-based R(t) element [21], the conductance of the element changes from a low to a high value within the charging periods of the capacitor and decays to a lower value within the slow discharging periods. R. Ivans et al. demonstrated the utility of CMOS-based R(t) circuits in conjunction with memristors to vary the resistance change with respect to time for implementing classical rate-dependent STDP [21]. In this approach, two identical R(t) elements were connected with the pre-and post-synaptic neurons to get a Hebbian asymmetric STDP. A significant reduction in complexity compared to pulse-shaping circuits is the benefit of including this component. Going further, a generic model explaining the time-dependent change in effective resistance of R(t) elements is required as a reference for establishing different synaptic learning behavior in SNNs.

This work explores a generic R(t) element model and its ability to generate different types of STDP functions. At this moment, it cannot be guaranteed that the model can consistently be implemented with standard CMOS circuitry. However, the model serves as a behavioral guideline for physical implementations [24]. Both classical and non-classical STDP learning behaviors from R(t)-based neural networks have been explored using TSMC 180 nm technology in this work. Furthermore, the network is tested with input spikes that are randomly generated using a Poisson process. The analysis in this paper can assist designers in understanding the dependency of the learning behavior of SNNs on different neuronal variables and parameters and thereby help design more accurate and efficient brain-emulating electronic circuits.

II. Neural Network Design

The SNN used in this work consists of a pre- and post-synaptic neuron connected together through a memristive synapse. This work analyzes a single memristive synapse connecting pre- and post-synaptic neurons via two R(t) elements on both sides of the synapse. Fig. 1. shows a

pseudo-schematic diagram of the SNN network building block used.

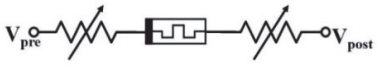

Fig. 1: Pseudo-schematic of a neural circuit with time-dependent resistance, or R(t) elements to control modification and learning in a memristive synapse [24].

The memristor and the R(t) elements are modeled in Verilog-A. Memory storage and processing happen inside the memristor, whose conductance defines the synaptic weight. The normalized conductance $\hat{\sigma}$ is calculated as the ratio of instantaneous conductance to the maximum conductance of the memristor and swings between 0 and 1. In this work, a non-linear drift model of a TiO_2-based memristor is used [2,25]. The memristor current is determined by an auxiliary circuit with a dependent current source and a 1 F capacitor. The voltage across the auxiliary capacitor modulates the memristor voltage and thus the conductance ($\hat{\sigma}$) of the device. The I-V characteristics, Verilog-A model of this memristor, and a more detailed description of parameters are provided in ref. [2].

III. Results & Discussion

Previous work has demonstrated learning in SNNs in which the R(t) element was either short-term charge-trapping memory or a circuit consisting of MOSFETs and resistors in which the effective resistance changes from a maximum to a minimum value [17,26]. To explore the ability of R(t) elements to generate different kinds of STDP learning rules, a generic model explaining the time-dependent change in effective resistance of R(t) elements is designed. This model serves as a reference for understanding the circuit parameters that regulate different synaptic learning behaviors in SNNs. The generic model of the R(t) element shown in Fig. 2 is designed in a way that the effective resistance is dependent on the input voltage and swings between a high resistance $R_{max}=1/\sigma_{min}$ and minimum resistance $R_{min}=1/\sigma_{max}$ [24].

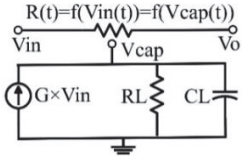

Fig. 2: Schematic of the generic model of R(t) element.

In this generic model, as the input to the circuit changes, the voltage across the capacitor changes due to charge injection by the dependent current source, and the conductance of the R(t) element changes based on equation (1). The effective resistance of the element can be equated as,

$$R(t) = \frac{1}{\sigma(t)} = f(\gamma(t)) \tag{1}$$

Here, γ is a time-dependent parameter that can be expressed as,

$$\gamma = \frac{V_{cap}(t)}{V_{cap}(max)} \tag{2}$$

where $V_{cap}(max)$ is the maximum capacitor voltage gained after charging for a duration of t_{charge}. This can be expressed as

$$V_{cap}(max) = \frac{(G \times Vdd \times t_{charge})}{C_l} \tag{3}$$

To physically implement an R(t) element following the generic model, a nanoscale transistor having low threshold and a linear current-gate voltage relationship in compatible technology is required. Further consideration is required to implement all the resistances with transistors.

Both classical and non-classical STDP are simulated using the SNN building block shown in Fig. 1. The details results are presented in the following subsections. Section III.A describes the R(t) function that can produce classical Hebbian STDP, while section III.B shows another R(t) function capable of producing Anti-Hebbian STDP. Finally, section III.C explains how the symmetric STDPs can be achieved using the R(t) function described in sections III.A and B.

A. Classical Hebbian STDP

To establish a classical Hebbian STDP learning behavior in the SNN, we need to formulate the conductance of the R(t) elements suitably. We denote the R(t) function that will be used for producing Hebbian STDP as $R_H(t)$. The conductance of $R_H(t)$ is equated as,

$$\sigma(t) = \sigma_H(t) = \sigma_{min} + \gamma \times \sigma_{max} \tag{4}$$

Effective conductance of the circuit was initially tested with a single pulse in TSMC 180 nm technology, as shown in Fig. 3. As the input to the circuit changes, the voltage across the capacitor changes exponentially. The conductance of the R(t) element exponentially changes from a maximum to a minimum value based on equation (4). For simulation, equations (1) to (4) were modeled in Verilog-A.

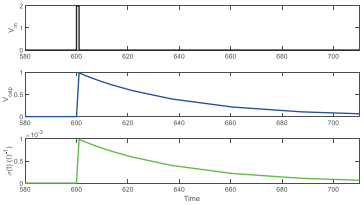

Fig. 3: Effective conductance of the $R_H(t)$ function with a single pulse input.

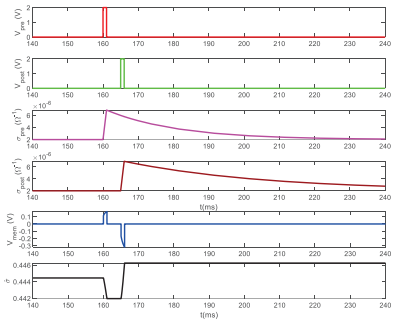

Fig. 4: Top to bottom: Pre-Post spike input pair voltages, instantaneous conductance of the pre-and post-synaptic R(t) circuits, memristor voltage, and memristor conductance change.

In order to establish a classical STDP learning behavior that follows the Hebbian rule, both the pre- and post-synaptic R(t) elements (Fig. 1) have identical $R_H(t)$. The network is analyzed with a single pair-based pre- and post-synaptic inputs which is presented in Fig. 4. For an initial normalized weight of 0.44, the voltage across the memristor changes during a 5 ms timing difference between pre-and post-synaptic signals. The normalized conductance $\hat{\sigma}$ changes accordingly within this time interval. The values used for constant parameters are given in Table I.

As shown in the middle traces of Fig. 4, the effective conductance for both pre-and post-synaptic neural circuits is plotted following the capacitor voltage. As the capacitor voltage decays exponentially with time after a pre-post pair, the conductance exponentially changes from a maximum to a minimum value. To verify the classical STDP, the weight change ($\Delta\hat{\sigma}$) across the memristor is plotted with respect to various timing differences (Δt) in Fig. 5. From this result, it is clear that STDP using the $R_H(t)$ function resembles biological classical (asymmetric) STDP behavior in Hebbian pattern.

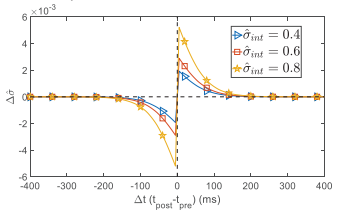

Fig. 5: Pair-based STDP with $R_H(t)$ function with R_{min}=200 kΩ and R_{max}=500 kΩ.

In a network, where neurons fire spikes randomly, the synaptic plasticity rule may go beyond the classical STDP. To verify the learning rule in a randomly spiked network, the R(t)-based network is fed by Poisson-distributed random pulse-train at both pre- and post-synaptic neuron and timing variations between spike pairs and the resulting weight changes are observed in Fig. 6(a)-(c).

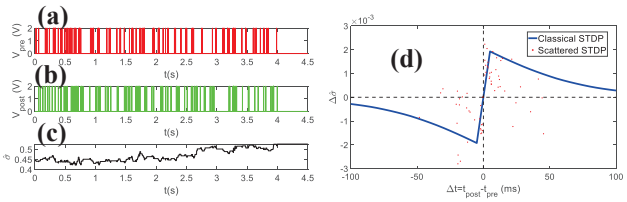

Fig. 6: (a) and (b) Timing of pre- and post-synaptic voltage spikes. (c) Weight change across the memristor due to random spiking inputs. (d) Scatter plot of a pair-based STDP curve calculated from the random spiking inputs.

The resulting STDP rule in Fig. 6(d) is calculated using the weight change due to a nearest-neighbor pre-post or post-pre pairs and the corresponding time difference between them. Since the data in Fig. 6(d) is very scattered, it demonstrates only moderate similarity to the classical Hebbian pair-based STDP measurements under the learning window (blue line). Scatter is primarily due to the fact that the calculation considers non-nearest-neighbor spike interactions regardless of the impact of the homogenous spikes [27]. These results also show that weight change does not follow classical Hebbian STDP purely.

TABLE 1. LIST OF PARAMETERS OF THE R(T) CIRCUIT

Parameters	Value
G ($\mu\Omega^{-1}$)	1
Δ t (ms)	5
C_L(pF)	1
R_{max}(kΩ)	100
R_{min}(kΩ)	1
V_{leak} (mV)	40
V_{th} (mV)	700
Vdd(V)	2

For further verification of the $R_H(t)$ function in memristive SNNs, the network was tested with multi-spike inputs, keeping the rate of pre- and post-synaptic signals identical. This experiment tests the effect of frequency of applied action potentials on the change in synaptic weight. Conductance change ($\Delta\hat{\sigma}$) of the memristor is plotted with respect to the inverse frequency (f^{-1}), i.e. the period of pre- or post-synaptic signals for three Δt values in Fig. 7. The other resistance values are kept same as Fig. 6. It is visible that this system demonstrates asymmetric temporal integration because the weight change is not constant for a given Δt.

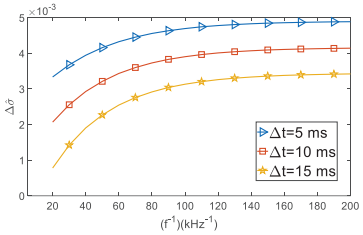

Fig. 7: Frequency dependence of synaptic weight change. Four action potentials are applied consecutively with an initial condition of $\hat{\sigma}$=0.5. The total weight change is measured as $\Delta\hat{\sigma}$.

B. Classical Anti-Hebbian STDP

The R(t) function that can be used to establish a classical Anti-Hebbian STDP learning behavior is termed $R_{aH}(t)$. The conductance of $R_{aH}(t)$ is equated as,

$$\sigma(t) = \sigma_{aH}(t) = \sigma_{min} + (\gamma - 1) \times \sigma_{max} \quad (5)$$

Following the same process followed with $R_H(t)$ function, we tested the effective conductance of the $R_{aH}(t)$ with a single pulse in TSMC 180 nm technology, as shown in Fig. 8. As the input to the circuit changes, the voltage across the capacitor changes exponentially. The conductance of the R(t) element exponentially changes from a maximum to a minimum value based on equation (5). Both the pre-and post-synaptic R(t) elements use the $R_{aH}(t)$ function in the neural network shown in Fig. 1. Conductrance change ($\Delta\hat{\sigma}$) across the memristor s plotted with respect to the timing difference (Δt) in Fig. 9 that resembles biological classical (asymmetric) STDP behavior in Anti-Hebbian pattern.

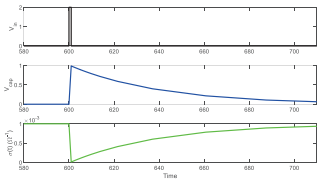

Fig. 8: Effective conductance of the $R_{aH}(t)$ function with a single pulse input.

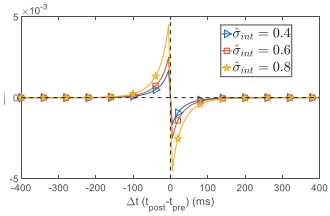

Fig. 9: Pair-based STDP with $R_{aH}(t)$ function with R_{min}=200 kΩ and R_{max}=500 kΩ.

C. *Non-Classical STDP*

Place figures and tables at the top and bottom of columns. Avoid placing them in the middle of columns. Large figures and tables may span across both columns. Figure captions should be below the figures; table heads should appear above the tables. Insert figures and tables after they are cited in the text. Use the abbreviation "Fig. 1", even at the beginning of a sentence. To generate non-classical i.e. symmetric STDP, non-identical R(t) functions are used with the pre- and post-synaptic neurons. The symmetric Hebbian STDP can be achieved by using RH(t) in the pre-synaptic neuron and RaH(T) in the post-synaptic neuron, as shown in Fig. 10(a) for different initial memristor conductance values. On the other hand, symmetric Anti-Hebbian STDP is generated by altering the R(t) functions from Hebbian STDP setup i.e. RaH(t) function in the pre-synaptic neuron and RH(t) function in the post-synaptic neuron, as presented in Fig. 10(b).

From Fig. 10(a) and (b), it is evident that the synaptic weight change for both positive and negative Δt has the same polarity; thus, they are symmetrical, which we call non-classical STDP. The magnitude depends on the tuning of the conductance of the R(t) elements. In Fig. 11, the symmetric Hebbian and Anti-Hebbian STDP are plotted as a function of Rmax and Rmin. The weight change across the memristor is calculated for three different minimum resistance values of the post-synaptic R(t) element. The other resistance values are kept the same as in Fig. 10. Fig. 11 shows that the STDP window can be shifted upwards or downwards along the vertical axis (Δσ), i.e. the potentiation and depression can be tuned by selecting the appropriate resistance values of the R(t) elements while the left-to-right symmetry remains intact.

IV. Conclusion

A generic model of R(t) elements was developed to tune the R(t) functions for establishing various STDP learning behavior in memristive SNNs. Both Hebbian and Anti-Hebbian STDP with corresponding R(t) functions were investigated, demonstrating clear asymmetric temporal integration and learning dependent on the timing and rate of the input spikes. Further investigation was done to appropriately apply the R(t) functions for obtaining symmetric or non-classical STDP. These analyses play the role of a guideline for implementing STDP-based supervised or unsupervised training of the SNNs with appropriate learning windows. The results of this work will be utilized to investigate more complex learning rules in the future. Furthermore, training and analysis of larger SNNs incorporating R(t) elements for the purposes of spatio-temporal pattern (STP) detection and classification.

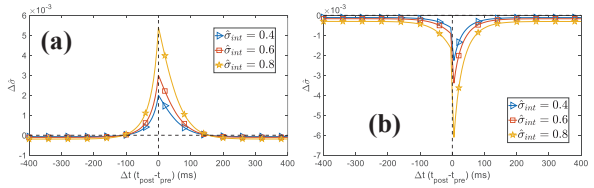

Fig. 10: (a) Symmetric Hebbian STDP, (b) Symmetric Anti-Hebbian STDP with R_{min}=200 kΩ and R_{max}=500 kΩ.

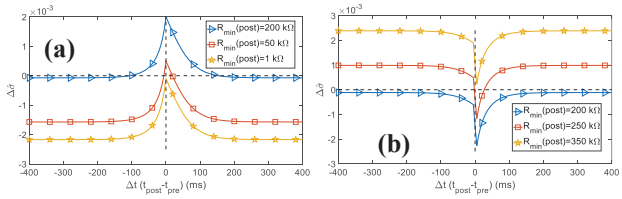

Fig. 11: (a) Symmetric Hebbian STDP, (b) Symmetric Anti-Hebbian STDP with different resistance conditions of R(t) elements.

Acknowledgment

Funding for this work is provided by the National Science Foundation award 1751230.

References

[1] M. Pfeiffer and T. Pfeil, "Deep Learning with Spiking Neurons: Opportunities and Challenges", Frontiers in Neuroscience, vol. 12, pp. 68–73, October 2018.

[2] S.G. Dahl, R.C. Ivans, & K.D. Cantley, "Effects of memristive synapse radiation interactions on learning in spiking neural networks", SN Appl. Sci., vol. 3, p. 555, 2021.

[3] Schuman, C.D., Kulkarni, S.R., Parsa, M. et al. Opportunities for neuromorphic computing algorithms and applications. Nat Comput Sci 2, 10–19 (2022).

[4] Davies, Mike, et al. "Loihi: A Neuromorphic Manycore Processor with On-Chip Learning." IEEE Micro (2018).

[5] K. A. Buchanan, "The activity requirements for spike timing-dependent plasticity in the hippocampus," Front. Syn. Neurosci., vol. 2, 2010, doi: 10.3389/fnsyn.2010.00011.

[6] H. Shouval, "Spike timing dependent plasticity: a consequence of more fundamental learning rules," Front. Comput. Neurosci., 2010, doi: 10.3389/fncom.2010.00019.

[7] C. Lammie, T. J. Hamilton, A. van Schaik and M. Rahimi Azghadi, "Efficient FPGA Implementations of Pair and Triplet-Based STDP for Neuromorphic Architectures," in IEEE Transactions on Circuits and Systems I: Regular Papers, vol. 66, no. 4, pp. 1558-1570, April 2019.

[8] Wang, Z., Zeng, T., Ren, Y. et al. Toward a generalized Bienenstock-Cooper-Munro rule for spatiotemporal learning via triplet-STDP in memristive devices. Nat Commun 11, 1510 (2020).

[9] Pfister, J.-P., & W. Gerstner, " Triplets of spikes in a model of spike timing-dependent plasticity," Journal of Neuroscience, vol. 26(38), pp. 9673–9682, 2006.

[10] J. Gjorgjieva, C. Clopath, J. Audet, J.-P Pfister, "A triplet spike-timing–dependent plasticity model generalizes the bienenstock–cooper–munro rule to higher-order spatiotemporal correlations," The Proceedings of the National Academy of Sciences (PNAS), vol. 108, pp. 19383–19388, USA, 2011.

[11] D. Krunglevicius. Modified STDP Triplet Rule Significantly Increases Neuron Training Stability in the Learning of Spatial Patterns. Advances in Artificial Neural Systems, 2016:1–12, aug 2016.

[12] Cai W, Ellinger F, Tetzlaff R. Neuronal synapse as a memristor: modeling pair- and triplet-based STDP rule. IEEE Trans Biomed Circuits Syst. 2015 Feb;9(1):87-95.

[13] PJ Sjöström, GG Turrigiano, SB. Nelson, "Rate, timing, and cooperativity jointly determine cortical synaptic plasticity," Neuron, vol. 32, pp. 1149-1164, Dec 2001.

[14] M. Prezioso, F.M Bayat, B. Hoskins, et al., "Self-Adaptive Spike-Time-Dependent Plasticity of Metal-Oxide Memristors," Scientific Reports, vol. 6, p. 21331, 2016.

[15] W. Wang, G. Pedretti, V. Milo, R. Carboni, A. Calderoni, N. Ramaswamy, A. S. Spinelli, D. Ielmini, "Learning of spatiotemporal patterns in a spiking neural network with resistive switching synapses," Science Advances, vol. 4, p. eaat4752, 2018.

[16] M. Prezioso, M.R. Mahmoodi, F.M. Bayat, et al., "Spike-timing-dependent plasticity learning of coincidence detection with passively integrated memristive circuits," Nature Communications, vol. 9, p. 5311, 2018.

[17] K. D. Cantley, A. Subramaniam, H. J. Stiegler, R. A. Chapman, and E. M. Vogel, "Spike timing-dependent synaptic plasticity using memristorsand nano-crystalline silicon tft memories," in *Proc. 11th IEEE Int. Conf. Nanotechnol.*, Portland, OR, USA, Aug. 2011, pp. 421–425.

[18] Bi, G. Q., and Poo, M. M. (1998). Synaptic modifications in cultured hippocampal neurons: dependence on spike timing, synaptic strength, and postsynaptic cell type. J. Neurosci. 18, 10464–10472.

[19] Henry Markram et al., Regulation of Synaptic Efficacy by Coincidence of Postsynaptic APs and EPSPs.Science275, 213-215(1997).DOI:10.1126/science.275.5297.213.

[20] Bliss TV, Lømo T. Long-lasting potentiation of synaptic transmission in the dentate area of the anaesthetized rabbit following stimulation of the perforant path. J Physiol. 1973 Aug;232(2):331-56. doi: 10.1113/jphysiol.1973.sp010273. PMID: 4727084; PMCID: PMC1350455.

[21] Hebb DO. The organization of behavior. New York: Wiley & Sons; 1949.

[22] Yang R, Huang H-M, Hong Q-H, et al. Synaptic suppression triplet-STDP learning rule realized in second-order memristors. Adv Funct Mater. 2018;28(5):1704455.

[23] R. Gopalakrishnan and A. Basu, "Triplet spike time dependent plasticity in a floating-gate synapse," 2015 IEEE International Symposium on Circuits and Systems (ISCAS), Lisbon, Portugal, 2015, pp. 710-713.

[24] F. Afrin and K. D. Cantley, "R(t)-Based Spike-Timing-Dependent Plasticity in Memristive Neural Networks," 2023 IEEE Workshop on Microelectronics and Electron Devices (WMED), Boise, ID, USA, 2023, pp. 1-4.

[25] Z. Biolek, D. Biolek, and V. Biolková, "SPICE model of memristor with nonlinear dopant drift," Radioengineering, vol. 18, no. 2, pp. 210–214, 2009.

[26] R. C. Ivans, S. G. Dahl, and K. D. Cantley, "A Model for R(t) Elements and R(t) -Based Spike-Timing-Dependent Plasticity with Basic Circuit Examples," IEEE Transactions on Neural Networks and Learning Systems, vol. 31, no. 10, pp. 4206-4216, Oct. 2020.

[27] K. D. Cantley, R. C. Ivans, A. Subramaniam and E. M. Vogel, "Spatio-temporal pattern recognition in neural circuits with memory-transistor-driven memristive synapses," 2017 International Joint Conference on Neural Networks (IJCNN), Anchorage, AK, USA, 2017, pp. 4633-4640.